energies

MDPI

Article

Effect of Solar Irradiation Inter-Annual Variability on PV and CSP Power Plants Production Capacity: Portugal Case-Study

Ailton M. Tavares [1,2,3], Ricardo Conceição [4], Francisco M. Lopes [5,6] and Hugo G. Silva [3,7,8,*]

1 Cátedra Energias Renováveis, IIFA, Universidade de Évora, Edifício Ário Lobo de Azevedo, Nossa Senhora da Tourega, 7000-083 Évora, Portugal; acmt@uevora.pt
2 Instituto de Ciências da Terra (ICT), IIFA, Universidade de Évora, Rua Romão Ramalho 59, 7002-554 Évora, Portugal
3 Laboratório Associado de Energia, Transporte e Aeronáutica (LAETA), Universidade de Évora, Rua Romão Ramalho 59, 7002-554 Évora, Portugal
4 High Temperature Processes Unit, IMDEA Energy, Avda. Ramón de La Sagra 3, 28935 Móstoles, Madrid, Spain; ricardo.conceicao@imdea.org
5 Instituto Dom Luiz (IDL), Faculdade de Ciências, Universidade de Lisboa, Campo Grande, 1749-016 Lisboa, Portugal; francisco.lopes@ipma.pt
6 Instituto Português do Mar e da Atmosfera (IPMA), Rua C ao Aeroporto, 1749-077 Lisboa, Portugal
7 Departamento de Física, ECT, Universidade de Évora, Rua Romão Ramalho 59, 7002-554 Évora, Portugal
8 INEGI Alentejo, Universidade de Évora, Largo dos Colegiais 2, 7000-803 Évora, Portugal
* Correspondence: hgsilva@uevora.pt

Abstract: The sizing of solar energy power plants is usually made using typical meteorological years, which disregards the inter-annual variability of the solar resource. Nevertheless, such variability is crucial for the bankability of these projects because it impacts on the production goals set at the time of the supply agreement. For that reason, this study aims to fill the gap in the existing literature and analyse the impact that solar resource variability has on solar power plant production as applied to the case of Portugal (southern Europe). To that end, 17 years (2003–2019) of meteorological data from a network of 90 ground stations hosted by the Portuguese Meteorological Service is examined. Annual capacity factor regarding photovoltaic (PV) and concentrating solar power (CSP) plants is computed using the System Advisor Model, used here for solar power performance simulations. In terms of results, while a long-term trend for increase in annual irradiation is found for Global Horizontal Irradiance (GHI) and Direct Normal Irradiance (DNI), 0.4148 and 3.2711 kWh/m^2/year, respectively, consistent with a solar brightening period, no corresponding trend is found for PV or CSP production. The latter is attributed to the long-term upward trend of 0.0231 °C/year in annual average ambient temperature, which contributes to PV and CSP efficiency reduction. Spatial analysis of inter-annual relative variability for GHI and DNI shows a reduction in variability from the north to the south of the country, as well as for the respective power plant productions. Particularly, for PV, inter-annual variability ranges between 2.45% and 12.07% in Faro and Santarém, respectively, while higher values are generally found for CSP, 3.71% in Faro and 16.04% in São Pedro de Moel. These results are a contribution to future instalments of PV and CSP systems in southern Portugal, a region with very favourable conditions for solar energy harvesting, due to the combination of high production capacity and low inter-annual variability.

Keywords: solar brightening; capacity factor; inter-annual variability; power plant performance; solar radiation

check for updates

Citation: Tavares, A.M.; Conceição, R.; Lopes, F.M.; Silva, H.G. Effect of Solar Irradiation Inter-Annual Variability on PV and CSP Power Plants Production Capacity: Portugal Case-Study. *Energies* **2024**, *17*, 5490. https://doi.org/10.3390/en17215490

Academic Editor: Tek-Tjing Lie

Received: 3 September 2024
Revised: 21 October 2024
Accepted: 26 October 2024
Published: 2 November 2024

Copyright: © 2024 by the authors. Licensee MDPI, Basel, Switzerland. This article is an open access article distributed under the terms and conditions of the Creative Commons Attribution (CC BY) license (https://creativecommons.org/licenses/by/4.0/).

1. Introduction

The migration to renewable energies, particularly in the field of Solar Energy, has been an important milestone for several countries that possess high solar resource irradiation. According to the latest statistics from the International Energy Agency (IEA), the contribution of photovoltaics (PVs) to the decarbonisation of the energy mix is in progress, reaching

a global installed capacity of ~1.2 TW in 2022, covering around 10% of global electricity demand and saving up to 1.399 million tons of CO_2eq [1]. Concentrating solar power (CSP), on the other hand, is seen as a promising technology to cope with solar intermittency due to its high storage capacity and energy dispatchability. The European Solar Thermal Electricity Association (ESTELA) predicts that CSP could provide around 4.500 TWh of solar thermal electricity by 2050, meeting up to 12% of global electricity demand [2]. As reliance on PV and CSP increases, it is crucial to examine their long-term reliability. These power plants are designed to operate for over 25 years, in which variations of Global Horizontal Irradiance (GHI) and Direct Normal Irradiance (DNI) introduce, respectively, uncertainties in PV and CSP production, particularly DNI, which is heavily cloud-influenced [3]. Indeed, long-term changes in solar irradiance due to solar dimming and solar brightening are evidenced [4–7]. These meteorological phenomena are characterised by a global decrease in surface solar radiation from 1961 to 1981 of about -3.07 W·m^{-2} per decade and a smaller increase from 1982 to 2019 of about +0.33 W·m^{-2} per decade [6]. According to Perdigão et al. [8], ground-based measurements in Portuguese stations during the period 1964–1989 show a downward trend in the incidence of global solar radiation until the mid-1970s, followed by an increase until the end of the studied period. This coincides with the dimming/brightening effects mentioned in the literature.

To the authors' best knowledge, there are few studies that have looked at the impact of global dimming and brightening [9] on the production of solar PV plants. Juruš et al. [10] presented a method for estimating the climatological variability of annual and monthly PV power production from 33 years of data. Results showed an apparent trend in annual PV production and significant evidence of brightening over Europe. Further studies are needed to understand how PV production may be affected by long-term variations in the surface solar resource. In another study, Perdigão et al. [8] analysed the variability and trends in global downward solar radiation over the Iberian Peninsula based on the ERA-40 reanalysis from 1964–1989. The authors examined observations from weather stations installed in Spain and Portugal over the same period. In Portugal, data from the stations of Lisbon, Porto, Faro, Évora and Bragança were used. From the latter, Faro and Évora showed relative GHI variability values of 3.6% and 4.9%, respectively. More recently, Bryce et al. [9] performed simulations to estimate the inter-annual variability of PV power generation in the Hawaiian archipelago using the System Advisor Model (SAM) [11], from the National Renewable Energy Laboratory (NREL), with 18 years of data from the National Solar Radiation Database. Results showed an inter-annual variability, based on the coefficient of variability (COV), with a variation in the order of 2% and 3% for the annual average GHI and the annual capacity factor (CF), respectively.

Regarding the impact of solar variability on CSP production, some authors highlight the importance of understanding how variations in DNI affect the operational efficiency and energy output of CSP plants [12,13]. Gueymard et al. [14] conducted a study on the long-term variability of aerosol optical depth (AOD), dust occurrence, and DNI over Kuwait. Both simulated and measured AOD datasets were used together with recorded DNI data from 1986 to 2016. The results indicated the presence of an upward trend in AOD over the past twenty years, with an annual increase of 0.0024. Consequently, this trend is expected to result in a decrease in available DNI resource of approximately 2%, which adversely impacts the long-term energy production of CSP plants. Martín-Pomares et al. [15] have analysed the long-term solar potential for electricity generation in Qatar using 11 years of hourly satellite-derived solar irradiance data. The authors performed simulations with the SAM, considering PV and CSP technologies; the analysis was focused on a parabolic trough with and without thermal storage, solar tower with molten salt and direct steam, a linear Fresnel, and a large flat plate PV grid-connected system. The results showed that parabolic trough with thermal storage, molten salt solar tower with large thermal storage, and grid-connected large PV systems offer low inter-annual variability, around 3%, and long-term stability for the produced electricity.

Moreover, it should be said that when a power supply contract is signed, it is usually estimated that the solar plant will deliver a certain amount of energy per year, based on a typical meteorological year (TMY). However, the inter-annual variability of the solar resource can lead to significant deviations between predicted and actual production. This uncertainty has a direct impact on energy production, which can result in the inability to meet contractual supply commitments. As a result, this variability not only threatens the reliability of the plant but can also have a negative financial impact on the return on investment. A thorough analysis of the variability of the solar resource is therefore essential to assess the financial risks and ensure the long-term economic viability of solar projects [9]. Furthermore, ensuring high annual irradiation and low variability of solar resources is crucial to the economic viability of these plants [16].

In a recent work, Tavares et al. [17] performed the assessment of modelled DNI and simulated CSP production capacity in mainland Portugal using TMY datasets. The study showed that some regions in Portugal, such as the southern (Alentejo and Algarve) and eastern central (Beira Interior) regions of Portugal, have very high potential for the installation of CSP solar power plants. Regional values for DNI annual irradiation were found to be above 2000 kWh/m^2/year, with CF values above 30%. Thus, it has already been demonstrated that these regions possess optimal conditions for the installation of solar power plants in terms of annual irradiation. However, it remains to be confirmed how the inter-annual variability of the solar resource impacts the long-term PV and CSP production. These details are crucial for the feasibility of the project and for forecasting the production of solar power plants. In fact, Silva et al. [18] previously found evidence that Alentejo and Algarve (southern Portugal) are the most suitable regions for the implementation of solar energy projects due to the combination of high average annual GHI irradiation and low inter-annual variability. In Sagres (the southernmost point of Portugal), the annual GHI irradiation reaches up to ~2028.4 kWh/m^2/year with 3.4% of inter-annual variability.

The present work provides more information on the variability of the solar resource in mainland Portugal by analysing the variability of DNI, particularly in the southern region of the country. Additionally, a comprehensive overview of how inter-annual variability in solar irradiance can affect the performance of solar power plants was also discussed. To this end, ground measurements of GHI were used, as well as other relevant meteorological variables (e.g., wind speed and ambient temperature); which are essential parameters for the simulation of solar power plants. In particular, the simulations of PV and CSP power plants were carried out using (as input) DNI modelled from GHI measurements. This model has already been validated by Tavares et al. [17]. This work initially showcases a long-term analysis of GHI and DNI annual irradiations and infers its impact on the production of PV and CSP power plants over a 17-year period (2003–2019). Subsequently, an evaluation is carried out over the inter-annual variability of both the solar resource and solar power production for the same period. A spatial analysis is performed to assess regions of lower variability. Hourly meteorological datasets from 90 ground stations, hosted by the Portuguese Meteorological Service ("Instituto Português do Mar e da Atmosfera"—IPMA), are used.

The remaining structure of this manuscript is described as follows: Section 2 presents the data and methodology used; results and respective discussions are shown in Section 3, while main conclusions and future work are provided in Section 4.

2. Data and Methodology

2.1. Measurements

GHI and other meteorological variables such as wind (speed and direction), atmospheric pressure, air temperature, and relative humidity were obtained from the IPMA's meteorological network, consisting of 90 stations spread across mainland Portugal. Details of the network can be found in previous works [17,18]. In this study, 17 years of data (from 2003 to 2019) have been used, measured on an hourly basis. Hourly measurements of GHI were made available using state-of-the-art instruments, namely the CM11 and Hukseflux

LP02 pyranometers, with the CM11 model being part of most of the IPMA stations. Both pyranometers are secondary standard instruments according to the International Organisation of Standardisation (ISO) 9060:1990 [19]. However, due to the large number of stations and their geographic distribution, there is no detailed information on their calibration and maintenance. Thus, in some cases, measurements may be affected by lack of calibration, malfunction, or, more commonly, soiling [20,21]. Among the other meteorological variables measured at the IPMA stations, air temperature and relative humidity are also used. These were recorded at a height of 1.5 m, from which hourly averages were considered for the present analysis; while wind speed was recorded at a height of 10 m, from which the averages of the last 10 min of each hour were considered [22]. Air temperature and relative humidity were measured with the Vaisala HMP45 sensor and wind speed was recorded with the Vaisala WAA 15A anemometer [23]. More detailed information regarding the geographical location of the 90 stations can be found in [17,18].

Time series data gaps were filled using methods similar to those commonly used in the literature, e.g., [17,18,24,25]. For GHI data gaps of one or two hours in a day, the missing values are filled in by linear interpolation from the non-missing values. For missing periods of three or more hours in a day, geographical interpolation is carried out. The latter algorithm begins by selecting the four neighbouring stations closest to the station for which the data gaps are to be filled and determines the long-term linear regression coefficients between this station and the neighbouring stations. With these four relationships, the hourly data gaps at the station are then filled by the median of the four hourly values of the values measured at the stations. The same procedure was followed for gap-filling in the time series of other meteorological variables. More information on the method can be found in [17,25].

DNI time series were estimated from observed GHI, measured at the referred stations. Engerer's deterministic model was used to calculate the DNI from the observed GHI. The DNI, Diffuse Horizontal Irradiance (DHI), and GHI, observations from a reference meteorological station at Évora, propriety of the Institute for Earth Science ("Instituto de Ciências da Terra"—ICT), were used to calibrate the parameters of the model [26]. This station is a high precision station having regular maintenance, and thus well fitted to perform this calibration. The calibrated parameters were then used for the estimation of DNI time series at all stations of the IPMA network. The estimated DNI time series were then reanalysed using a Multivariate Regression Model (MRM2, [17,27]). The MRM2 model consists of combining several meteorological datasets as input, from which the best combination between these leads to a reduction of the bias between observed and modelled DNI. The observed DNI is used together with the abovementioned meteorological data to calibrate the MRM2 model parameters. The complete methodology for obtaining DNI values from meteorological measurements can be found in detail in previous work [17]. The values obtained for the annual DNI irradiations are consistent with observations in the south of Portugal [28], validating the model.

Measurements of GHI and DHI at the ICT station were carried out with pyranometers (model CMP11), which are secondary class instruments [19]. The DHI was measured using a pyranometer with a shadow ball to block the direct solar radiation. Reference observations of DNI in the ICT station were made using a CHP1 pyrheliometer, a World Meteorological Organisation (WMO)-class instrument [29]. Generally, these solar instruments are mounted on a SOLYS2 Sun-Tracker (Kipp & Zonen) [27]. For more information on measurements carried out at IPMA and ICT stations, as well as the adopted filters applied to the raw data, please see [17,18,24,25,29].

2.2. Capacity Factor

The annual capacity factor is the ratio of the usable power generated in one year to the power that would have been generated if the system had been operating at full capacity for the same period [30–32]. The CF of power plants indicates both the amount of the local resource in terms of irradiance and the characteristics of the atmospheric conditions that

may attenuate solar power conversion at a given location. This makes it a very useful metric for comparing solar power plants across different locations and time scales. In this work, the CF is calculated for both PV and CSP plants by means of the power plant simulator, the SAM (version 2017.9.5). The model allows not only to obtain performance predictions, but also energy cost estimates that these systems require [11]. The formula for the CF is presented in Equation (1):

$$CF = \frac{Annual\ Energy\ Produced}{Maximum\ energy\ that\ could\ be\ produced} = \frac{Annual\ Energy\ Produced}{P_n \times (8760\ h)}, \quad (1)$$

in which P_n is the nominal power of the power plant, in the present case, $P_n \cong 50$ MW. It is remarked that presenting the CF is equivalent to present the annual energy production as this can be determined using the previous equation.

2.3. PV Power Plant Model

A 50 MW PV system simulation model is made available with the SAM, namely the PVWatts, being simulated at each ground station location. Following the usual standard for PV installation, the latitude of the location in which the analysed stations are installed is considered, as well as the PV tilt angle. The simulation parameters are listed below:

1. Nominal power: 50 MWdc;
2. Module type: standard;
3. DC to AC ratio: 1.2;
4. Rated inverter size: 41.6 MWac;
5. Inverter efficiency: 96%;
6. Array type: fixed open rack;
7. Tilt angle: local latitude (L) for each station;
8. Azimuth: 180;
9. Ground coverage ratio: 0.4;
10. System loss: soiling—0%; shading—3%; mismatch—2%; connections—0.5%; light-induced degradation—1.5%; nameplate—1%; age—0%; availability—3%; total system losses—12.32%.

2.4. CSP Power Plant Model

The SAM is also used to simulate a CSP plant and estimate its production capacity using meteorological data from IPMA. This exercise focuses on a case study of an operational CSP plant with similar configurations to Andasol 3 (Granada, southern Spain), based on the model previously developed in [31,33]. The Andasol 3 is a commercial power plant based on a linear focus parabolic trough system, with thermal oil as the heat transfer fluid, using an indirect molten salt storage capacity of 7.5 h at full load. Its solar field aperture area is 510,120 m^2, with a nominal capacity of 50 MWe and an expected power generation of 175 GWh/year. Further information on the power plant configuration can be found in [34].

2.5. Coefficient of Variability

To characterise the distribution of inter-annual variability for each station, the coefficient of variability (COV) of the annual irradiation for GHI and DNI, as well as the CF for PV and CSP plants, were all calculated. The COV is defined as the percentage of the standard deviation of the annual irradiations, or the CF values, relatively to the annual irradiation, or the CF values, averaged for all years of the time-series, as described in [9,35]:

$$COV = \frac{\sigma}{\overline{x}} \times 100\%\ , \quad (2)$$

where σ is the standard deviation for inter-annual variation and $\overline{x}$ is the mean average of N years. In summary, for each station, the annual time series of meteorological data

are generated and analysed, out of which the annual irradiation values of GHI and DNI are assessed. The SAM is then employed to compute the annual CF for PV (CF_{PV}) and CSP (CF_{CSP}). This process is systematically applied across all stations. Finally, a COV is calculated for each variable analysed (GHI, DNI, CF_{PV}, and CF_{CSP}) in each station.

3. Results and Discussion

3.1. Temporal Evolution of Annual Solar Irradiation and CF

Figure 1 shows the temporal evolution of annual irradiation over 17 years (2003 to 2019) at four IPMA stations (Lisboa, Sines, Beja, and Faro). All stations analysed showed an upward trend in solar irradiation, which is more significant for the DNI, particularly in Lisbon with a noticeable increase (~14 kWh/m^2/year), than for GHI (~4 kWh/m^2/year). The GHI average annual irradiation values for the IPMA stations were approximately 1796.88, 1864.16, 1886.54, and 1942.92 kWh/m^2/year, respectively. Regarding the average annual irradiation of DNI, the corresponding values found were 2048.13, 2140.06, 2086.83, and 2249.88 kWh/m^2/year, respectively. These average values are consistent with the values found from the TMY analysis [17].

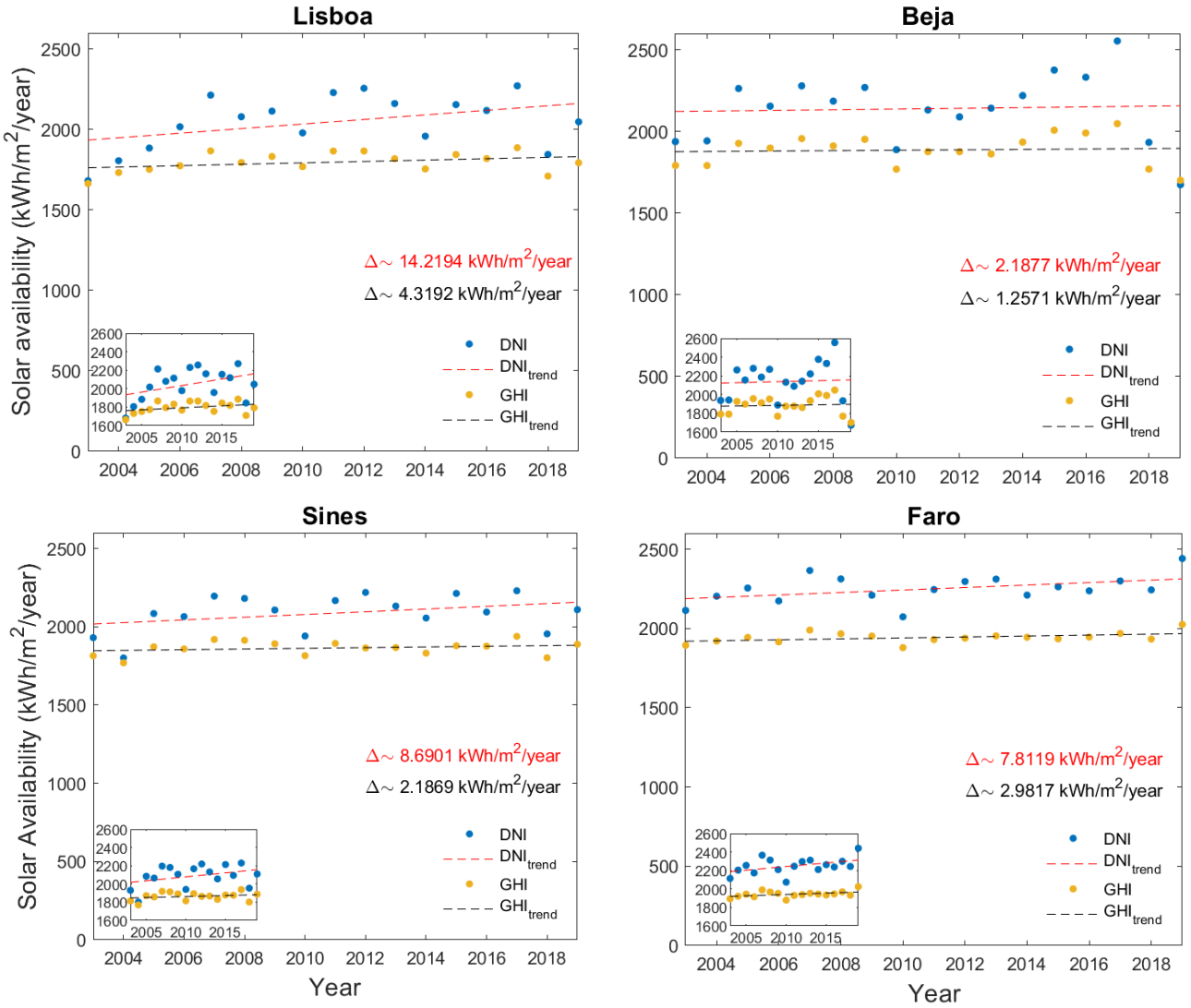


Figure 1. Temporal evolution of DNI (blue dots) and GHI (yellow dots) annual irradiation from 2003 to 2019 at four reference IPMA stations: Lisbon, Beja, Sines, and Faro. Dashed lines are the trends, inside plots show the data inset.

Similarly, in Figure 2, the CF results are shown for both simulated PV and CSP plants, each with an installed nominal capacity of 50 MWe over a period of 17 years. Despite the upward trend in solar resource irradiation, the same behaviour is not observed in the capacity factor CF of PV and CSP power plants. Nevertheless, CSP shows a slightly higher tendency to increase over the years in relation to PV, although not significant. For instance, in Lisbon, the CF_{CSP} shows a tendency of increase ~0.002%/year, while the CF_{PV} shows a tendency of increase ~0.0005%/year. Additional factors, such as the effects of rising temperatures, which can adversely affect the efficiency of solar energy conversion, may be responsible for this phenomenon. This will be discussed in more detail further on. Moreover, average CF values are shown to be of 17.90, 17.96, 18.22, and 19.39% for PV in Lisboa, Beja, Sines, and Faro, respectively. Conversely, for CSP, the average CF values are significantly higher, 30.87, 31.38, 32.48, and 35.79%, respectively. These values are consistent with the average CF values found for CSP from the TMY analysis [17].

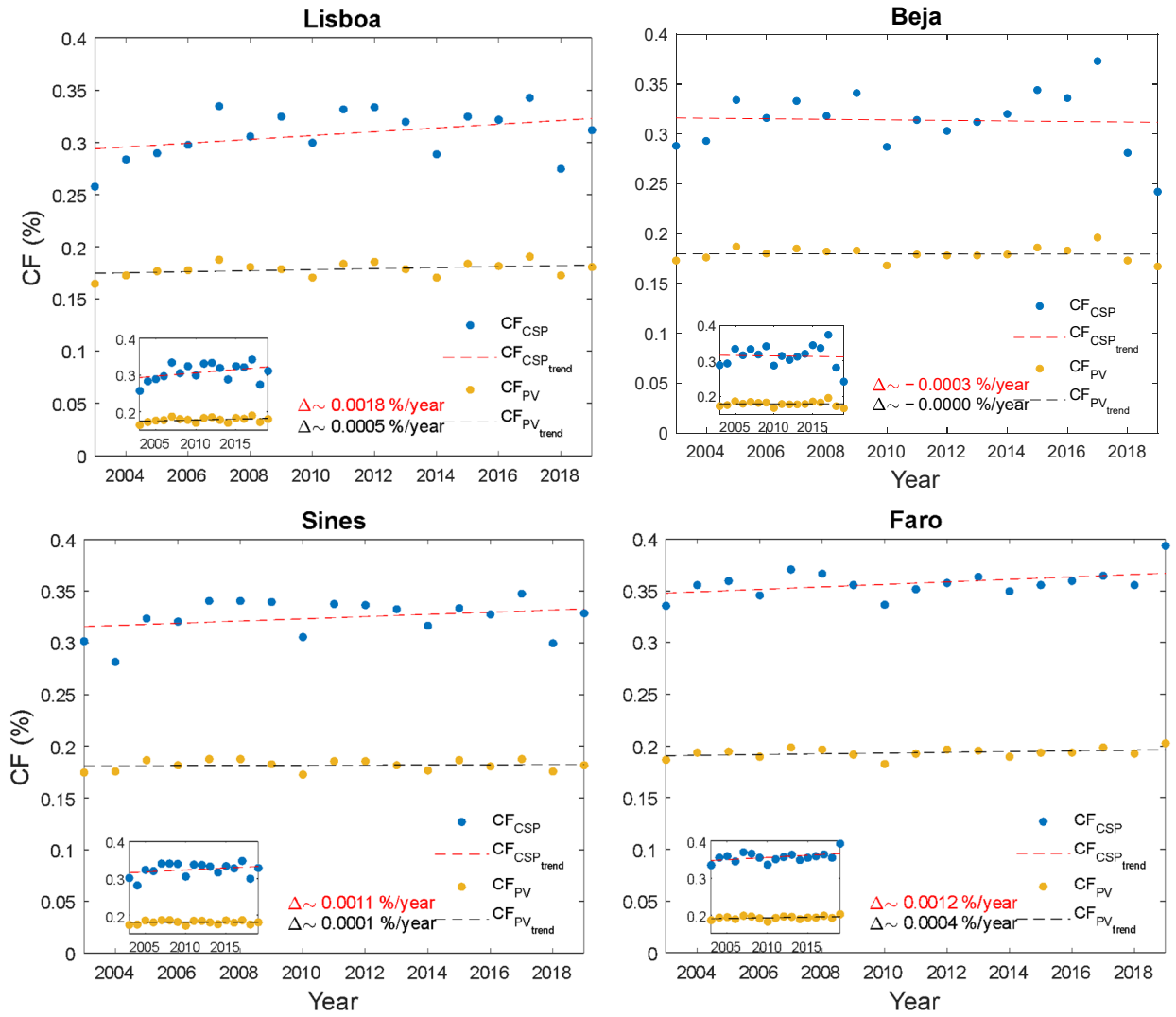


Figure 2. Temporal evolution of the capacity factor of CSP (blue dots) and PV (yellow dots) plants from 2003 to 2019 at four IPMA stations: Lisbon, Beja, Sines, and Faro. Dashed lines are the trends, inside plots shows the data inset.

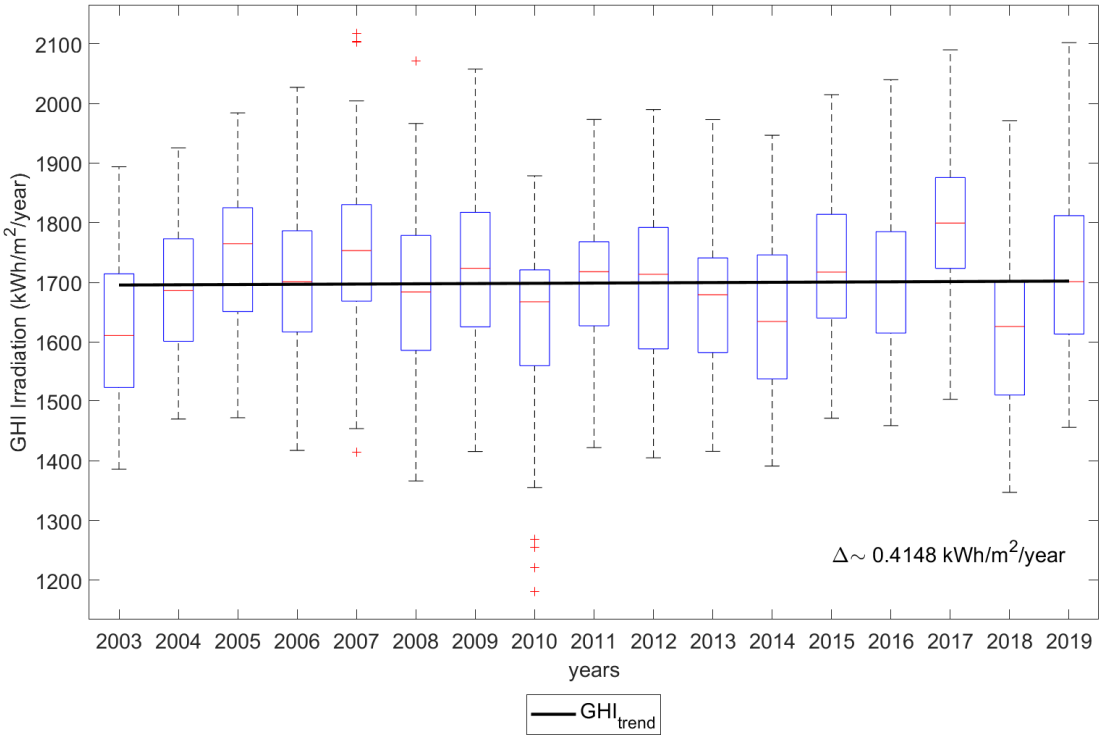
Figure 3 shows an analysis at the regional scale of the temporal evolution of GHI and DNI annual irradiation, the CF for PV and CSP plants, as well as the ambient temperature (Ta) at the 90 IPMA stations over the considered period. Each boxplot shows for each year the error distribution of the considered parameters (GHI, DNI, CF_{PV}, CF_{CSP}, and Ta) for all the stations studied. The analysis shows an increasing trend (based on the median of the annual data from all stations) in GHI annual irradiation of ~0.41 kWh/m^2/year, Figure 3a. This implies a gradual increase in the amount of solar irradiance measured at the stations over time. Additionally, a significant annual increase in the DNI irradiation (~3.27 kWh/m^2/year) can be seen in Figure 3b. This growth is significantly higher compared to the GHI behaviour. The discrepancy in growth rates between DNI and GHI highlights the importance of considering both parameters when assessing the solar potential of a region. The tendencies observed for GHI and DNI irradiation seem to confirm the occurrence of a solar brightening period, which is a significant result in the present analysis that needs to be highlighted. Moreover, Figures 3c and 3d show the temporal evolution of CF for PV and CSP plants, respectively. The data did not reveal any significant trends of increase or decrease in CF for either PV or CSP technologies. This indicates that other operational or environmental factors may influence the respective performance indicator, suggesting that the increase in solar resource irradiation, both GHI and DNI, may not reflect on the CF of the solar power plants. In fact, the analysis of the temporal evolution of Ta in Figure 3e shows an increasing trend of ~0.02 °C/year (roughly ~0.4 °C during the period in consideration). The gradual rise in temperature could substantially affect the CF_{PV} and CF_{CSP}. The increase in Ta and the stability of CF may indicate that despite an increase in the annual irradiation, the efficiency of solar power plants could be adversely affected by rising temperatures. Such behaviour is easily explained for PV, as it is well established that temperature affects semiconductors by increasing charge carrier recombination and reducing the photovoltaic effect [36]. This finding is consistent with the study presented by Todorović et al. [37], where the authors analysed the performance of a grid-connected photovoltaic system over a 10-year period under temperate continental conditions in Serbia, concluding that the system behaviour remained essentially constant over this period. However, for CSP, the effect of ambient temperature increase over plant efficiency is more complex, as it may result from the increase of the temperature at which heat is rejected in the Rankine cycle that will reduce the overall cycle's efficiency [38]. The efficiency of a heat engine can be approximated to:

$$\eta = \eta_{ex}\eta_{Carnot} = \eta_{ex}(1 - T_L/T_H), \quad (3)$$

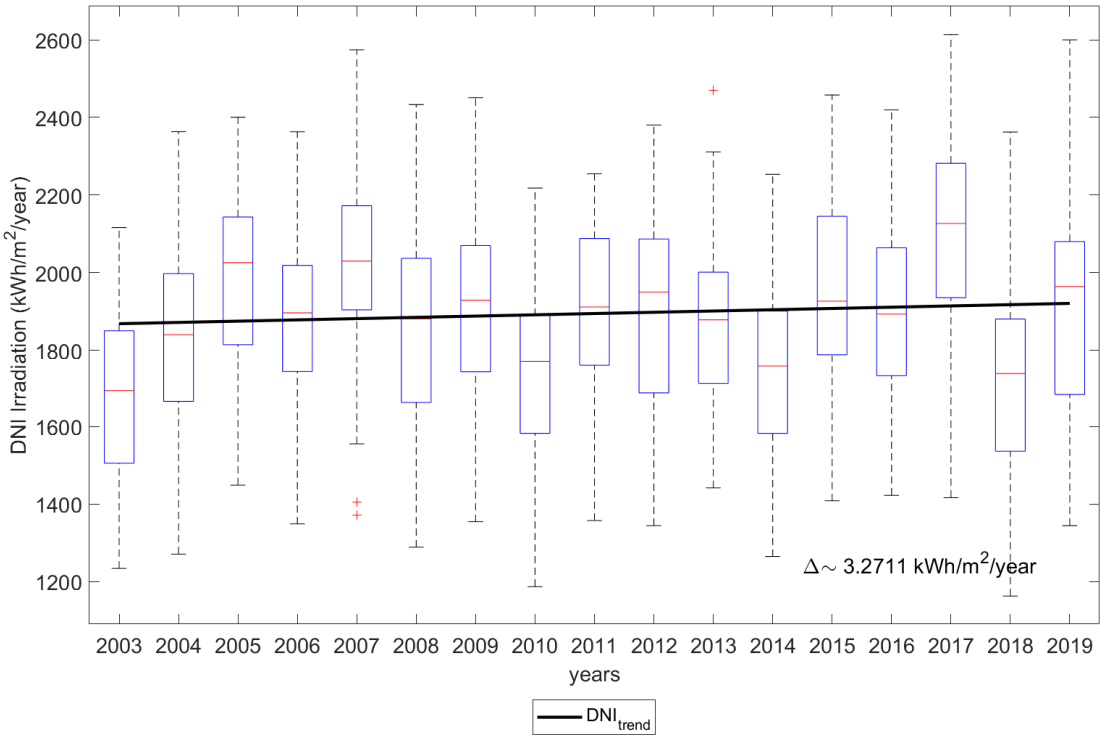
where η_{ex} is the exergetic efficiency, typically ~0.6–0.7, T_L is the absolute temperature of the heat output reservoir (that is the ambient air in dry-cooling power plants), and T_H is the absolute temperature of the heat input reservoir. From this equation it can be stated that higher T_L leads to lower efficiency.

3.2. Correlation Between Annual Irradiation and Power Plants Production

Figure 4 presents the correlation between GHI and DNI annual irradiation and CF respectively for PV and CSP power plants. The results show a good correlation between annual irradiation and production in both cases, of about 95%. The very low *p*-values (<0.001) show that the production of the PV and CSP plants is strongly correlated with the irradiation of the GHI and DNI, respectively.

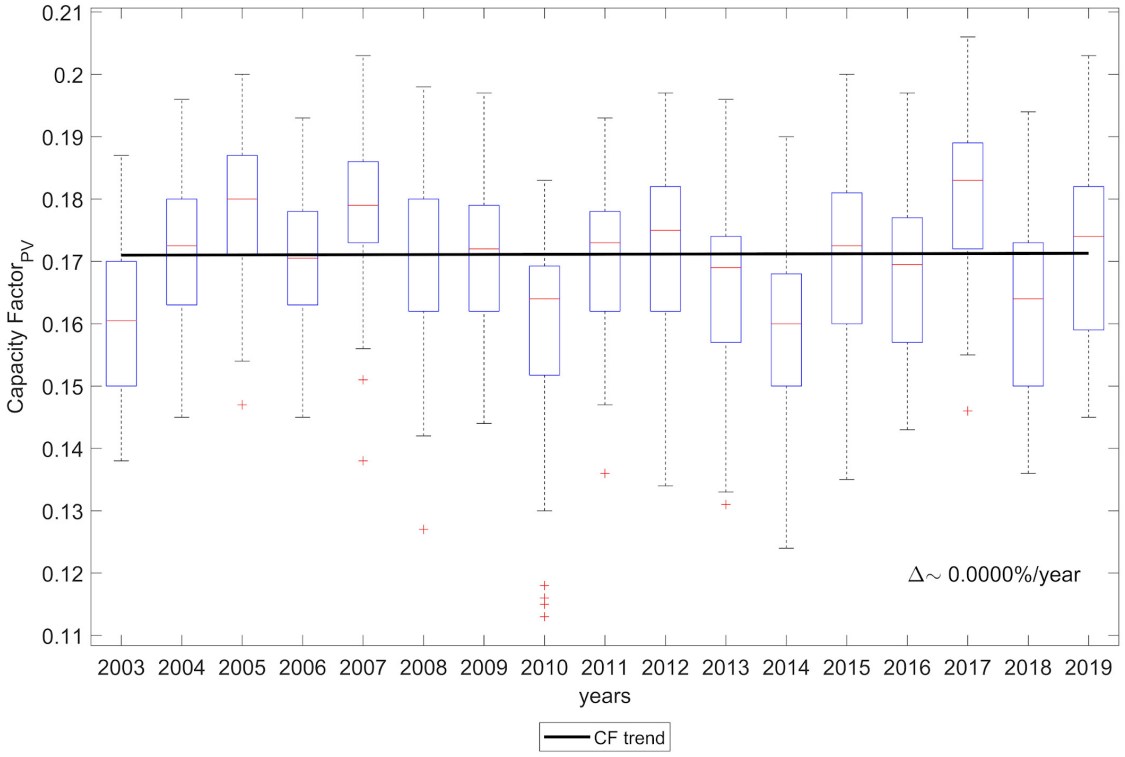


(**a**)

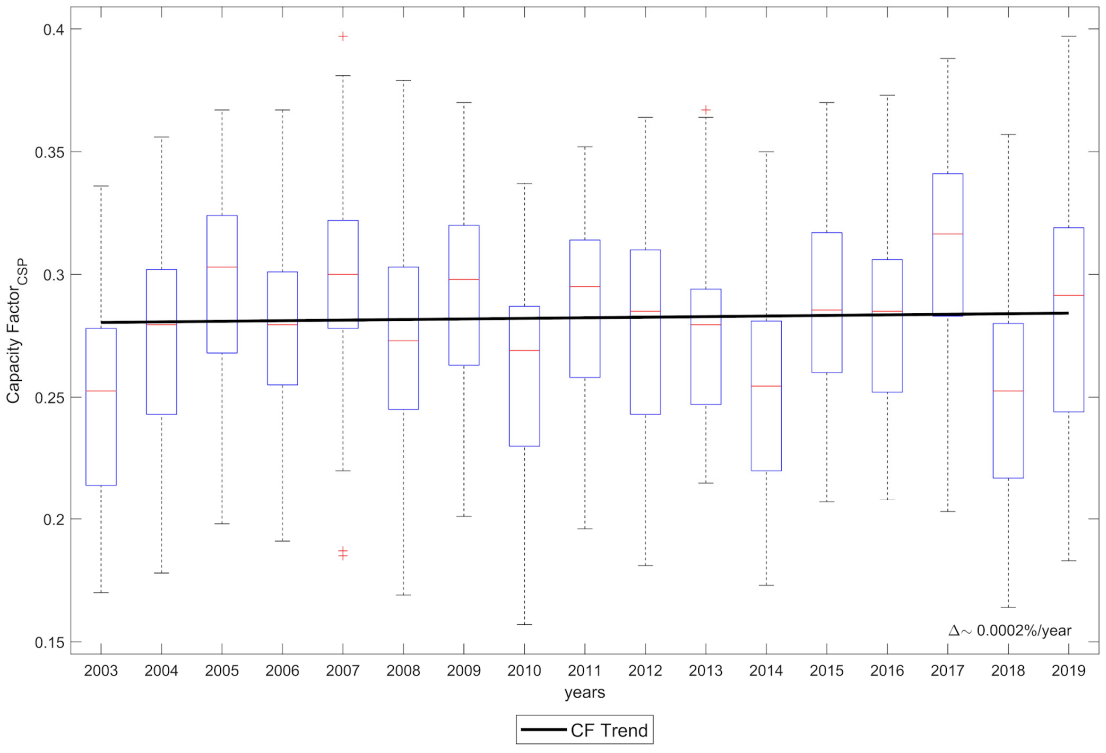


(**b**)

Figure 3. *Cont.*

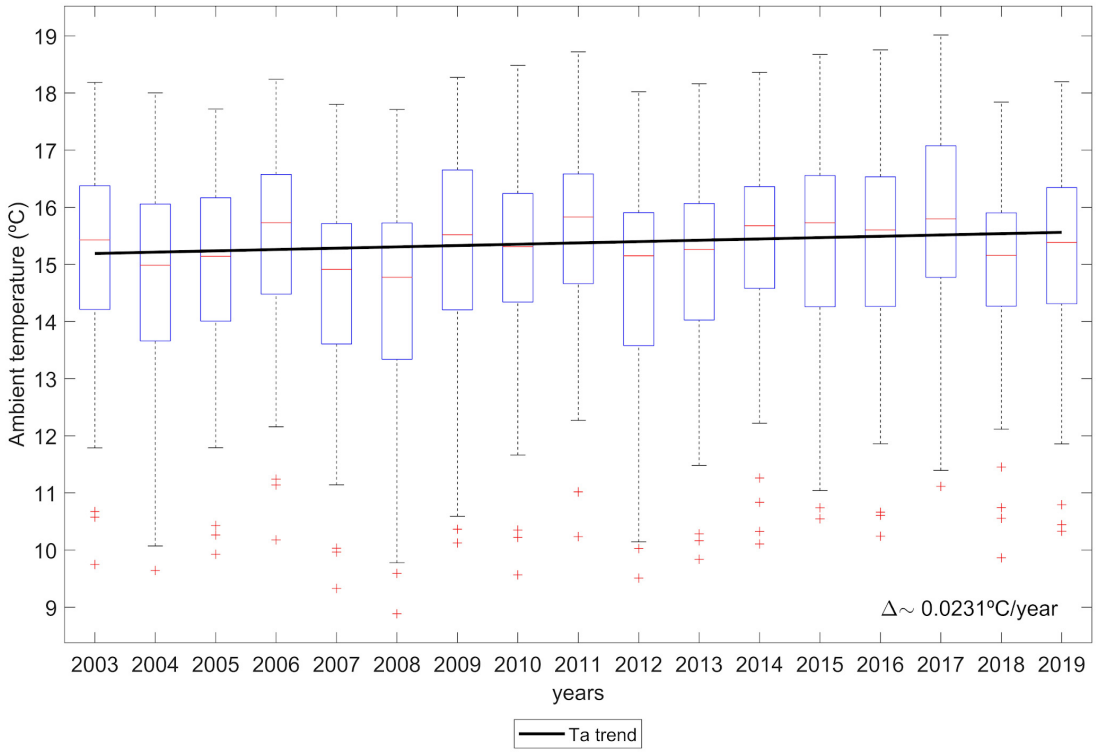


(**c**)



(**d**)

Figure 3. *Cont.*



(**e**)

Figure 3. Boxplots with the temporal evolution at 90 IPMA stations over a 17-year period, from 2003 to 2019 of: (**a**) GHI irradiation, (**b**) DNI irradiation, (**c**) CF for PV plant, (**d**) CF for CSP plant, and (**e**) ambient temperature, Ta. The median is represented by a red line in each boxplot, the red crosses are outliers, and the black straight line shows the trend of the median.

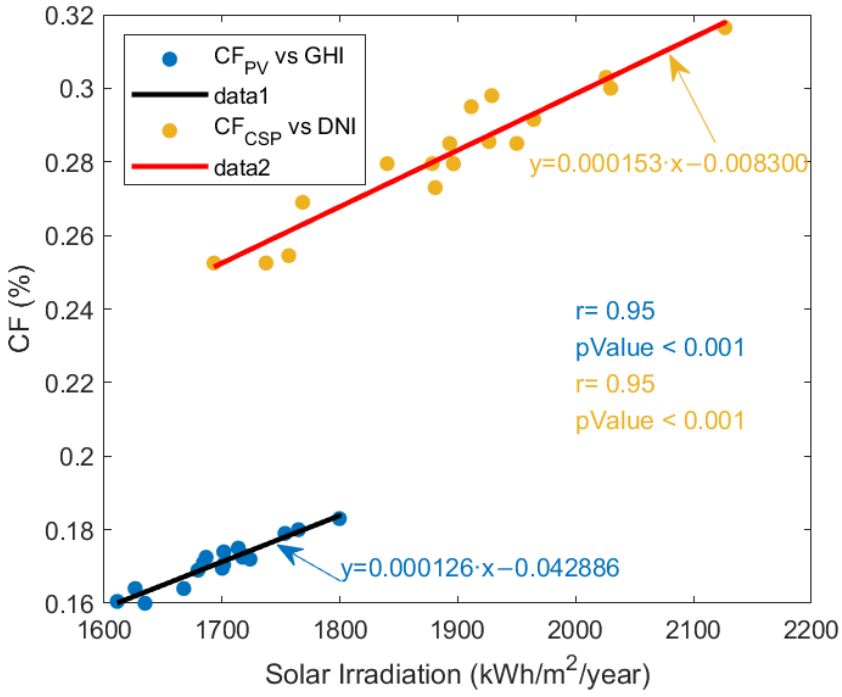


Figure 4. Correlation between annual irradiation and CF of the solar power plants. The CF_{PV} is correlated with the GHI irradiation (blue dots) and the CF_{CSP} is correlated with the DNI irradiation (yellow dots). The trends are shown by solid lines.

3.3. Spatial Distribution of GHI and DNI Variability

Having analysed the long-term tendencies of the solar resource and its impact on solar power plants production capacity, the spatial distribution of GHI and DNI inter-annual variability is now focused. Particularly, for mainland Portugal (Figure 5), as indicated by the previously defined COV parameter at the IPMA stations, a kriging technique was applied to generate interpolated maps (similarly to previous works [17,18]). COV values for GHI, Figure 5a, show a decrease from north to south of the country, corresponding with an increase of GHI irradiation. In Alentejo (south-central region), GHI variability ranges from 2.32% (4.20%) in Odemira, more towards the coast, to 6.40% (1.14%) in Reguengos. In Algarve (southernmost region), the inter-annual variability of GHI ranges from 1.75% (1.05%) in Faro to 3.82% (1.32%) in Portimão. It is worth noting that the differences between these results are the ones obtained in [18], i.e., the ones in parentheses, and can be attributed to the use of 20 years of data in the latter study, whereas only 17 years were used in the present one.

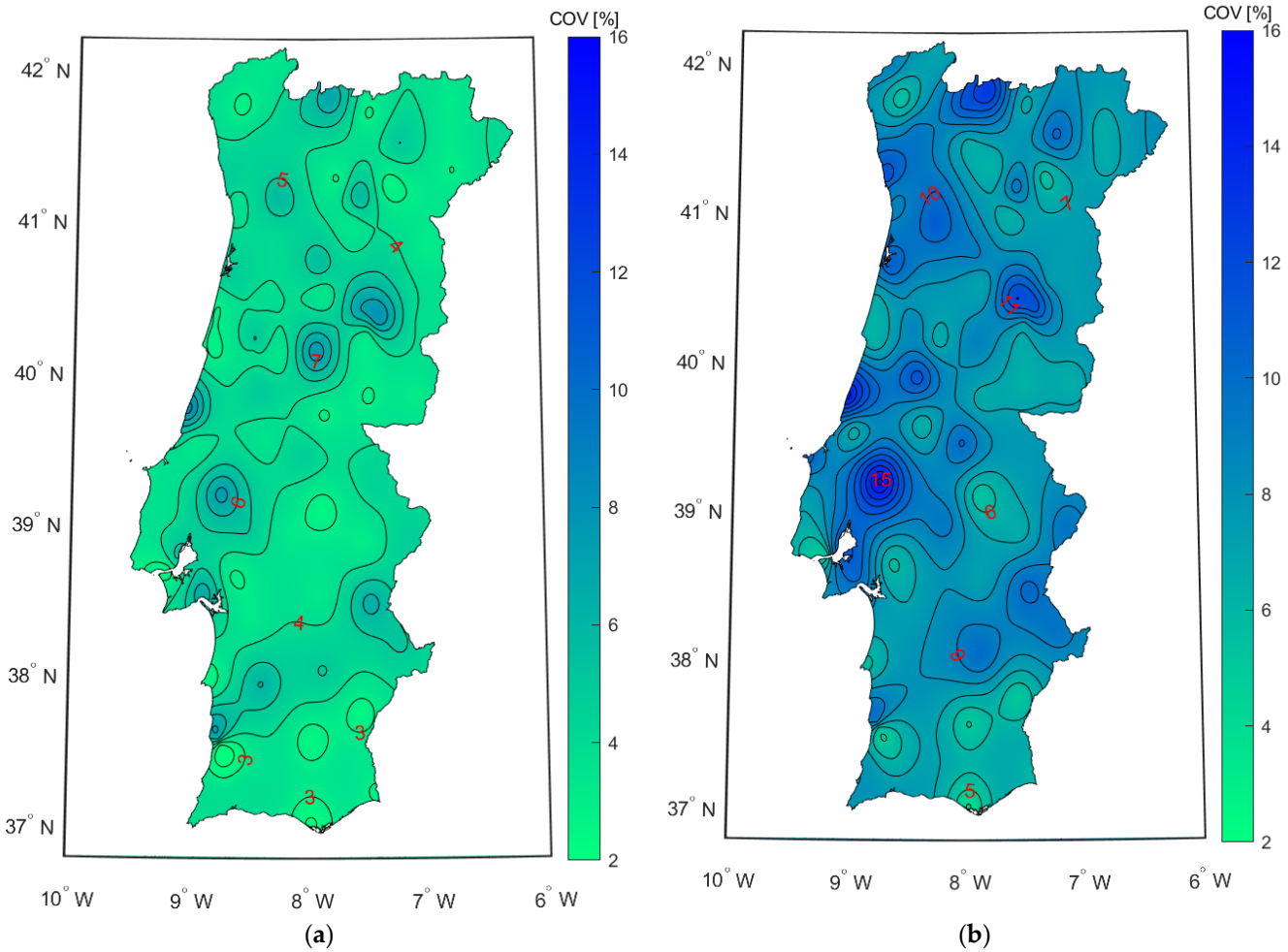


Figure 5. Comparison of variability in annual irradiation: (**a**) GHI, (**b**) DNI.

Regarding DNI, in Figure 5b, the COV for the annual irradiation across mainland Portugal follows a similar pattern to the one found for GHI. Variability is lower in southern Portugal, especially in Algarve region, with values ranging from 3.90% in Faro to 7.81% in Sagres. The latter is the southernmost station used in the present study, where the lowest variability is found (similarly to GHI). In Alentejo region, the DNI variability ranges from 4.94% in Castro Verde, closer to Algarve, to 10.30% in Reguengos. As expected, the DNI

variability in the annual irradiation is larger than that of GHI, having a more significant impact on power plant production for CSP in comparison to PV.

3.4. Spatial Distribution of PV and CSP Variabilities

Figure 6 shows the relative CF variability for PV (CF_{PV}) and CSP (CF_{CSP}) plants over the 17-year period. The analysis is performed based on the CF value (Equation (1)) obtained through the SAM output. Again, a kriging technique was applied to generate interpolated maps with calculated CF variability. The impact of the inter-annual variability of GHI on the CF for PV systems is also discussed here using the COV (Figure 6a). Similarly, to the previous variability maps of GHI irradiation, the CF_{PV} variability for PV is lower in the south (Algarve), where the COV ranges from 2.45% in Faro to 4.28% in Sagres. In Alentejo, the CF variability for PV is lower in Sines, around 2.81%, while being higher in Zambujeira, around 7.18%. In general, lower values of COV for CF_{PV} can be found more towards the south of the country. This is in accordance with previous studies [17,18,39], where high levels of annual solar resource irradiation are to be found in this region.

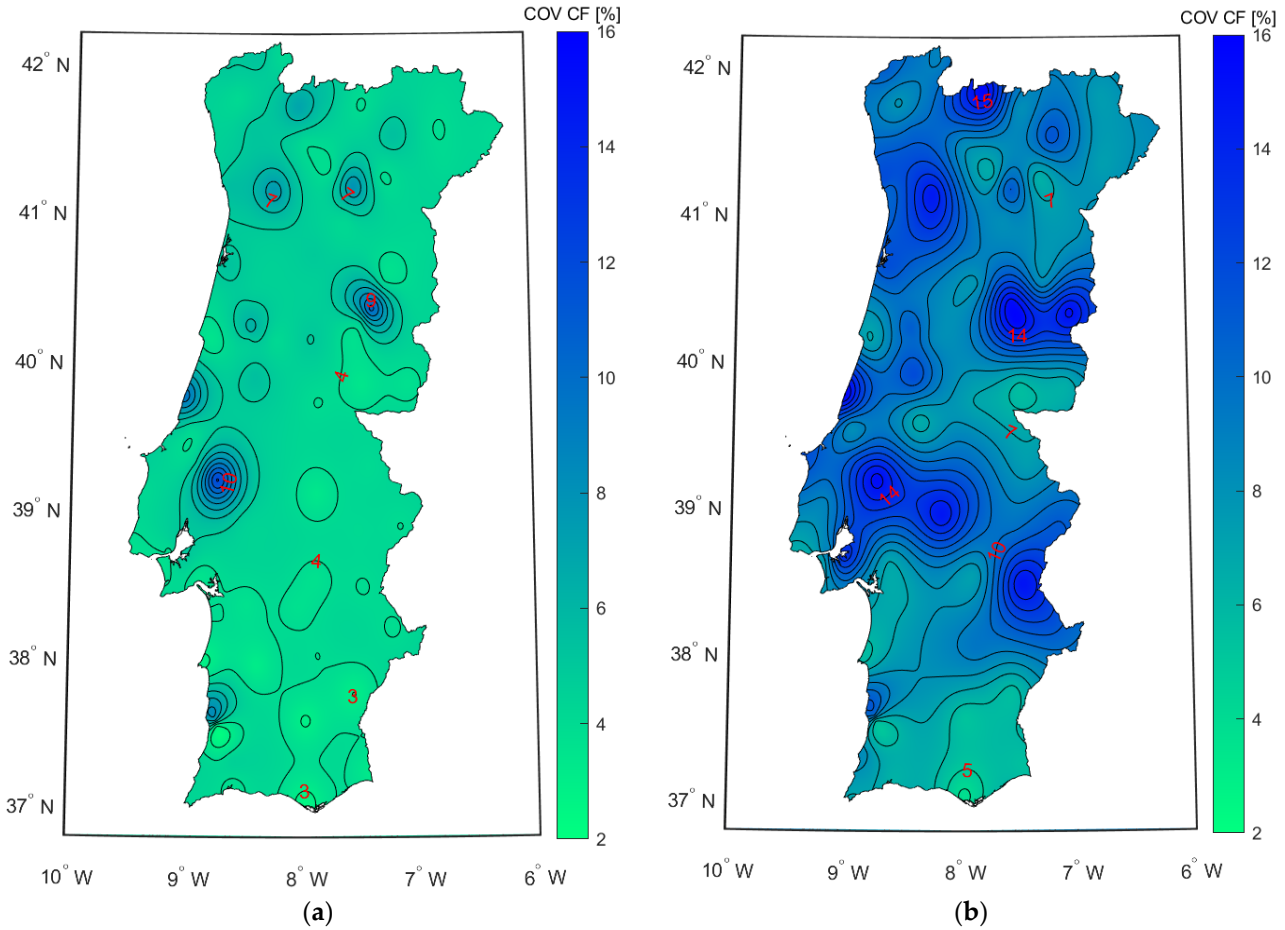


Figure 6. Comparison of capacity factor variability for mainland Portugal: (**a**) PV, (**b**) CSP.

Regarding the assessment of the CF_{CSP}, shown in Figure 6b, it can be observed that COVs for CF_{CSP} are higher than for the CF_{PV}, following a similar trend as DNI related with GHI. Moreover, from north to south, there is a tendency for the CF_{CSP} variability to be reduced. As a matter of fact, in the southern region of Portugal, the variability of the CF_{CSP} is lower in Faro, around 3.71%, and higher in Aljezur, around 8.00%. Additionally, in Alentejo, the relative variability of CF_{CSP} is lower in Castro Verde, around 5.34%, and higher in Reguengos, around 14.91%.

Information on the location, altitude, years of available irradiation data, and other relevant details for all stations used in this study can be found in Appendix A.

3.5. Discussion

From the results presented above, Alentejo and Algarve, the southern regions of Portugal, offer exceptional conditions for the implementation of PV and CSP power plants. Such evidence was shown as result of the combination of significant values for respective plant production: CF_{PV} above 18% and CF_{CSP} above 30%, as well as low inter-annual variabilities, below 8% and 14%, respectively. These values are good indicators for investors and make these regions very attractive to receive investments in these technologies. For potential investors in the solar industry and policy makers, this information can be very useful, since the observed low variability of the solar resource suggests a more predictable and consistent energy output from solar power plants, which is essential for energy planning and the assurance of return on investment in solar energy projects.

It should be noted that Portugal possesses a national plan for energy and climate (PNEC 2030) [40], for the decade 2021–2030, towards carbon neutrality. This plan sets an ambitious target that aims to a strong incorporation of renewable energies in the energy sector (around 47%). As a contribution to this aspect, the present work can be used as a tool by providing concrete guidelines for regions of great interest for the installation of both PV and CSP systems.

4. Conclusions

An analysis towards CF variation for two types of simulated power plants, a CSP and a PV system, was carried out over a period of 17 years (from 2003 to 2019) for mainland Portugal. Although the present study was conducted using data from Portugal, other climate regions are eligible for the same type of study. Observed hourly GHI, air temperature, relative humidity, atmospheric pressure, and wind speed were collected from a network comprising 90 ground stations hosted by the Portuguese Meteorological Service–IPMA. In addition, DNI estimates were calculated from GHI measurements using the Engerer model and reanalysed using the Multivariable Regression Model from all observed meteorological data. With the available datasets, power plant performance simulations were carried out using the SAM for the CSP plant and the PV plant, both with a nominal power of 50 MWe. For the proposed procedures, the COV was used for each plant's CF variability over the entire period of study.

The annual irradiation of GHI and DNI shows a long-term upward trend, increasing by 0.4148 and 3.2711 $kWh/m^2/year$, respectively, clearly evidencing a period of solar brightening. However, in terms of CF, there is no discernible trend for either for PV or CSP generation despite the solar radiation trend. This indicates that the increased annual irradiation of GHI and DNI is not reflected in the production levels of PV and CSP systems, which is likely due to the parallel increase in ambient temperature at a rate of 0.0231 $^{\circ}C/year$.

A spatial distribution analysis was also performed for the annual irradiation and power plants CF variabilities. The presence of a downward tendency was observed, following a north to south direction, in mainland Portugal. This decrease in variability is accompanied by an increase in the irradiation and CF, which implies that the regions with higher production capacity also have lower production variability.

The present results indicate that the Alentejo and Algarve regions in southern Portugal have very favourable conditions for the implementation of solar energy, due to their high irradiation and production capacity and low inter-annual variability.

Further studies will examine the influence of storage capacity on the variability of power plant production. This research seeks to explain the extent to which increasing storage capacity can mitigate the variability inherent in energy production, thus increasing the stability and reliability of these power plants.

Author Contributions: Conceptualization, R.C. and H.G.S.; Methodology, F.M.L.; Validation, R.C. and H.G.S.; Formal analysis, A.M.T. and H.G.S.; Investigation, A.M.T.; Data curation, A.M.T.; Writing—original draft, A.M.T.; Writing—review & editing, R.C., F.M.L. and H.G.S.; Visualization, R.C. and F.M.L.; Supervision, H.G.S. All authors have read and agreed to the published version of the manuscript.

Funding: This research was funded by the European Union through the European Regional Development Fund, framed in COMPETE 2020 (Operational Programme Competitiveness and Internationalisation) through "Fundação para a Ciência e a Tecnologia" Base Funding: ICT—UIDB/04683/2020 and LAETA—UIDB/50022/2020.

Data Availability Statement: The data presented in this study are available on request from the corresponding author.

Acknowledgments: The authors are thankful to IPMA and ICT for providing solar radiation data from their measuring networks to perform this study. A.M.T. thanks the Millennium BCP foundation and the Camoes I.P. for their financial support. Ailton Tavares also thanks ICT, LAETA, and the Renewable Energies Chair of the University of Évora. R.C. acknowledges the Juan de la Cierva Formación 2020 program, reference FJC2020-043159-I, funded by MCIN/AEI/10.13039/501100011033 and by the European Union NextGenerationEU/PRTR. R.C. also acknowledges the grant PID2020-119403RB-C21 (HECTOR), funded by MCIN/AEI/10.13039/501100011033. F.M.L. acknowledges the funding of IPMA in the framework of the Horizon Europe CERISE project (N.º 9227/2023). H.G.S. acknowledges the Physics Department of the University of Évora for supporting his work and the discussions on this topic held with Jorge Neto, Afonso Cavaco, Paulo Canhoto, and Manuel Collares-Pereira.

Conflicts of Interest: The authors declare no conflict of interest.

Appendix A

Table A1. List of all IPMA stations (latitude, longitude, elevation, years of available data, annual DNI and GHI irradiation from TMY, PV and CSP capacity factor, and COV).

Station Names	Lat. (°N)	Lon. (°W)	Elev (m)	Period (years)	E_b (kWh/m^2/year)	E_g (kWh/m^2/year)	CF_mean PV(%)	CF_mean CSP (%)	COV GHI (%)	COV CF PV (%)	COV DNI (%)	COV CF CSP (%)
Cabo Carvoeiro/Farol	39.36	−9.41	32.00	9.01	1521.87	1625.36	16.98	25.23	3.37	4.78	10.74	11.97
Sagres/Quartel da Marinha	37.01	−8.95	22.85	10.02	2245.30	1988.94	19.18	36.09	3.64	4.28	7.81	6.90
Lisboa/Geofísico	38.72	−9.15	77.00	13.30	1888.81	1755.44	17.90	30.87	4.10	3.80	8.30	8.64
Sines/Monte Chãos	37.95	−8.84	103.00	19.72	2024.39	1854.89	18.22	32.48	2.53	2.81	5.75	5.86
Viana do Castelo/Meadela	41.71	−8.80	16.00	4.79	----------	---------	----------	----------	--------	---------	--------	---------
Porto/Pedras Rubras	41.23	−8.68	69.00	17.63	1624.47	1603.49	16.45	26.21	6.08	5.18	11.35	11.75
Coimbra/Aeródromo	40.16	−8.47	171.00	17.01	1809.43	1645.21	16.26	25.38	4.12	5.08	8.42	10.30
Faro/Aeroporto	37.02	−7.97	5.00	16.96	2280.66	1963.54	19.39	35.79	1.75	2.45	3.90	3.71
Évora/Aeródromo	38.54	−7.89	247.56	13.21	2030.14	1808.25	18.32	31.79	3.84	3.65	7.18	7.28
Viseu/Aeródromo	40.71	−7.90	644.37	13.97	1786.90	1622.90	17.09	28.12	6.18	4.91	9.09	9.03
Beja	38.03	−7.87	246.00	17.02	2145.45	1878.65	17.96	31.38	4.76	3.99	9.98	9.46
Vila Real/Aeródromo	41.27	−7.72	561.00	19.92	1603.01	1561.46	15.25	24.02	3.01	4.26	6.41	6.80
Penhas Douradas/Observatório	40.41	−7.56	1380.00	14.80	1467.85	1672.30	15.37	23.47	17.33	6.79	11.92	15.25
Castelo Branco	39.84	−7.48	386.00	11.83	2078.07	1769.59	18.26	32.22	14.59	3.41	6.24	5.82
Portalegre	39.29	−7.42	597.00	17.07	1875.37	1698.47	16.98	28.52	4.46	4.05	7.63	7.34
Bragança	41.80	−6.74	690.00	17.57	1847.01	1648.14	16.98	28.81	3.59	4.18	7.34	7.43
Lisboa/Gago Coutinho	38.77	−9.13	103.88	17.14	1985.18	1788.31	17.66	30.17	5.07	4.52	9.72	9.57
Odemira/S.Teotónio	37.55	−8.73	120.54	15.92	2051.54	1825.73	18.36	31.84	2.31	3.42	5.91	6.23
Vila Nova de Cerveira/Aeródromo	41.97	−8.68	34.00	15.30	1618.96	1532.58	15.74	24.17	4.43	5.00	8.85	10.69
Monção/Valinha	42.07	−8.38	80.00	15.14	1555.61	1466.69	14.84	21.38	3.59	5.31	7.44	9.48
Lamas de Mouro	42.04	−8.20	880.00	15.12	1553.14	1464.82	15.20	21.83	3.79	4.22	7.09	8.93
Montalegre	41.82	−7.79	1005.00	15.78	1262.83	1383.36	14.95	21.18	6.73	5.43	12.98	15.61
Ponte de Lima/Escola Agrícola	41.76	−8.57	40.00	17.20	1538.06	1518.47	14.79	21.66	3.11	4.11	5.36	7.87

Table A1. *Cont.*

Station Names	Lat. (°N)	Lon. (°W)	Elev (m)	Period (years)	E_b (kWh/m^2/year)	E_g (kWh/m^2/year)	CF_mean PV(%)	CF_mean CSP (%)	COV GHI (%)	COV CF PV (%)	COV DNI (%)	COV CF CSP (%)
Chaves/Aeródromo	41.73	−7.47	360.00	17.97	1627.84	1568.18	15.10	23.43	3.35	3.92	6.77	8.25
Cabril/S. Lourenço	41.71	−8.03	585.00	6.70	1460.30	1458.28	14.96	22.69	4.78	6.93	11.03	12.29
Braga/Merelim	41.58	−8.45	68.35	16.30	1725.64	1571.64	15.82	25.12	4.59	5.15	9.18	10.25
Cabeceiras de Basto	41.49	−7.98	350.00	16.99	1549.57	1521.93	15.13	23.42	4.24	4.19	6.89	8.52
Mirandela	41.51	−7.19	250.00	13.33	1704.56	1597.46	16.27	27.11	5.31	5.44	10.16	11.28
Macedo de Cavaleiros/Izeda-Morais	41.57	−6.79	702.00	13.51	1991.53	1679.19	17.42	29.72	3.65	3.93	6.53	7.85
Miranda do Douro	41.50	−6.27	693.00	12.72	1992.55	1709.17	17.55	30.15	4.68	4.08	8.24	8.27
Mogadouro	41.34	−6.73	644.00	17.08	1973.36	1685.47	17.45	28.73	3.15	4.09	6.62	7.31
Carrazêda de Ansiães	41.24	−7.30	715.00	16.97	1665.29	1574.04	16.48	26.08	2.80	4.02	5.66	6.40
Porto/S.Gens	41.18	−8.64	89.19	6.81	1630.00	1543.47	15.99	25.31	5.32	5.61	9.77	10.79
Moncorvo	41.19	−7.02	600.00	17.04	1889.45	1662.77	16.58	27.48	3.35	4.38	7.10	7.89
Pinhão	41.17	−7.55	130.00	9.92	1508.15	1535.83	15.27	23.64	5.42	7.93	9.38	11.01
Luzim	41.15	−8.25	287.17	9.39	1510.18	1492.18	15.20	21.59	5.81	7.58	10	14.6
Moimenta da Beira	40.99	−7.60	715.00	16.80	1776.39	1633.02	16.04	24.55	3.41	4.53	6.36	8.37
Trancoso/Bandarra	40.78	−7.35	840.00	15.89	1931.57	1692.99	17.45	29.25	4.70	4.30	7.63	8.15
Arouca	40.93	−8.26	270.00	5.88	1775.57	1612.02	15.87	23.98	5.60	5.22	10.86	13.25
Figueira de Castelo Rodrigo/V.Torpim	40.83	−6.94	635.00	16.23	1843.46	1653.39	17.26	28.11	3.23	4.19	7.35	8.07
Guarda	40.53	−7.28	1020.00	16.13	2111.23	1734.55	17.80	30.67	5.98	4.27	7.97	8.43
Nelas	40.52	−7.86	425.00	16.07	1745.60	1580.33	17.00	27.20	17.24	4.66	7.06	7.94
Pampilhosa da Serra	40.15	−7.93	835.59	13.55	1918.11	1664.43	17.25	29.07	16.58	5.04	8.85	8.84
Covilhã	40.26	−7.48	482.00	14.41	2090.86	1738.84	17.82	31.29	10.25	4.98	7.84	15.65
Aldeia Souto/Quinta Lageosa	40.35	−7.39	468.00	7.93	1824.67	1647.52	15.88	25.74	12.07	10.24	11.36	14.03
Lousã/Aeródromo	40.14	−8.24	193.77	11.85	1608.49	1555.31	15.37	22.48	8.33	4.20	6.66	8.56
Aveiro/Universidade	40.64	−8.66	5.00	17.79	1607.61	1586.50	16.68	25.99	5.91	5.30	10.62	11.64
Dunas de Mira	40.45	−8.76	14.00	7.57	1510.74	1535.10	15.91	23.12	3.34	4.41	6.98	9.21
Anadia/Estação Vitivinícola da Bairrada	40.44	−8.44	45.00	17.48	1399.34	1487.32	15.09	21.86	3.88	4.80	7.74	9.49
Coimbra/Bencanta	40.21	−8.46	35.00	10.22	1691.03	1593.23	15.75	23.09	4.99	6.20	8.77	10.85
Figueira da Foz/Vila Verde	40.14	−8.81	4.00	16.50	1963.77	1717.17	17.08	27.69	3.11	3.52	6.24	6.98
Ansião	39.90	−8.41	396.24	15.01	1721.54	1612.64	16.25	24.01	4.88	5.47	11.41	11.81
Leiria/Aeródromo	39.78	−8.82	45.00	11.38	1573.39	1567.91	16.05	23.96	4.82	5.92	10.8	11.42
Leiria/Barosa	39.75	−8.83	24.00	4.14	----------	----------	----------	----------	--------	----------	-------	----------
São Pedro de Moel	39.76	−9.03	40.00	9.15	1917.07	1675.57	16.28	24.01	8.48	9.63	14.31	16.04
Tomar/Vale Donas	39.59	−8.37	75.42	15.94	1860.74	1710.12	16.54	27.78	3.54	4.72	6.42	6.60
Alcobaça/Estação Fruticultura Vieira Natividade	39.55	−8.97	38.00	16.66	1781.07	1669.28	16.75	26.68	3.50	4.40	6.79	8.31
Rio Maior/ETAR	39.31	−8.92	52.83	14.55	1692.12	1648.63	16.29	25.41	4.54	5.09	10.4	11.93
Santarém	39.20	−8.74	71.91	17.04	1522.67	1554.56	15.56	25.98	6.97	12.07	15.19	15.37
Torres Vedras/Dois Portos	39.04	−9.18	110.00	16.05	1924.50	1726.04	17.26	27.46	3.73	4.60	8.43	8.94
Coruche/Estação de Regadio (INIA)	38.94	−8.51	18.75	16.15	2115.38	1825.18	17.82	31.00	6.49	4.75	9.10	12.06
Santa Cruz/Aeródromo	39.13	−9.38	40.71	8.81	1889.36	1703.69	17.69	28.12	4.53	4.16	7.52	10.12
Cabo da Roca	38.78	−9.50	141.23	6.68	1893.25	1695.90	16.43	20.31	8.65	6.91	25.9	35.98
Lisboa/Tapada da Ajuda	38.71	−9.18	69.96	8.90	1861.28	1722.95	17.16	28.55	3.93	3.99	5.92	8.82
Cabo Raso/Farol	38.71	−9.49	7.88	9.63	2218.63	1847.57	19.04	33.65	3.71	3.62	6.39	6.73
Barreiro/Lavradio	38.67	−9.05	6.00	16.04	1604.73	1649.61	16.58	25.35	3.90	4.97	10.85	13.43
Pegões	38.65	−8.64	64.00	6.80	2044.33	1810.87	17.26	29.39	2.99	4.36	5.85	7.18
Setúbal/Estação de Fruticultura	38.55	−8.89	35.00	16.06	1963.72	1769.06	17.49	30.55	6.85	3.56	9.90	9.71
Almada/Praia da Rainha	38.62	−9.21	5.51	16.63	1885.80	1743.98	17.82	30.48	3.46	3.60	6.69	7.03
Alcácer do Sal/Barrosinha	38.36	−8.48	29.00	16.49	1999.84	1801.29	17.69	29.78	3.08	3.65	7.10	6.91
Alvalade	37.95	−8.39	46.97	15.37	1838.25	1740.06	17.35	29.81	5.70	3.08	7.99	7.92
Zambujeira	37.58	−8.74	67.00	9.79	1901.81	1769.89	17.48	29.36	5.47	7.18	8.76	9.87
Aljezur	37.33	−8.80	11.95	13.79	1931.27	1787.92	17.88	30.95	3.21	4.09	7.40	8
Foia	37.31	−8.60	895.30	8.67	2213.31	1809.38	18.71	31.56	3.21	4.53	6.23	6.47
Sabugal/Martim Rei	40.34	−7.04	858.00	14.39	2067.15	1749.23	17.98	30.58	10.15	4.44	7.33	15.2
Zebreira	39.85	−7.07	374.00	15.48	1963.11	1742.58	17.78	30.45	3.11	3.69	6.40	6.54
Proença-a-Nova/Moitas	39.73	−7.87	379.00	14.73	2069.83	1751.58	17.74	30.58	13.03	3.97	6.71	6.93
Alvega	39.46	−8.03	51.05	15.87	1836.80	1693.62	17.08	28.38	4.65	4.28	10.09	8.94
Avis/Benavila	39.11	−7.88	152.25	16.30	1986.54	1753.16	17.28	28.96	4.87	3.32	5.37	11.2
Mora	38.94	−8.16	129.45	6.41	1730.08	1670.45	15.61	23.00	5.93	4.34	9.44	14.78

Table A1. *Cont.*

Station Names	Lat. (°N)	Lon. (°W)	Elev (m)	Period (years)	E_b (kWh/m^2/year)	E_g (kWh/m^2/year)	CF_mean PV(%)	CF_mean CSP (%)	COV GHI (%)	COV CF PV (%)	COV DNI (%)	COV CF CSP (%)
Elvas/Est. Melhoramento Plantas	38.89	−7.14	209.97	16.71	2127.34	1815.76	18.29	32.67	6.30	3.98	9.69	11.09
Estremoz/Techocas	38.86	−7.51	366.00	16.31	2198.18	1845.04	18.54	32.57	5.12	4.11	6.58	9.89
Reguengos/S.Pedro do Corval	38.48	−7.47	265.17	9.39	1905.44	1744.70	17.48	28.79	7.82	3.93	10.3	14.91
Viana do Alentejo	38.33	−8.05	202.00	8.66	1890.40	1724.96	17.91	29.44	4.01	3.69	8.58	7.98
Amareleja	38.21	−7.21	192.00	9.45	1996.22	1798.38	17.65	30.84	6.71	3.89	9.68	11.62
Amareleja2	38.20	−7.23	180.00	4.58	----------	----------	----------	----------	-------	-------	-------	---------
Mértola/Vale Formoso	37.76	−7.55	190.00	15.54	2044.28	1802.03	17.88	30.62	2.46	2.97	5.07	5.73
Castro Verde/Neves Corvo	37.58	−7.97	225.00	17.13	1882.23	1779.48	17.84	29.51	2.26	2.86	4.94	5.34
Castro Marim/Reserva Nacional do Sapal	37.23	−7.43	4.83	16.57	2310.08	1912.79	19.32	35.35	2.83	3.23	6.08	5.50
Portimão/Aeródromo	37.15	−8.58	2.00	16.19	2196.05	1882.81	18.58	33.88	3.83	3.75	7.44	6.23

References

1. International Energy Agency. Snapshot 2023. Available online: https://iea-pvps.org/snapshot-reports/snapshot-2023/ (accessed on 2 February 2024).
2. European Solar Thermal Electricity Association. The Value of Solar Thermal Electricity. 2016. Available online: https://www.estelasolar.org/Docs/2016_ESTELA_STE-CSP_Value_Final.pdf (accessed on 25 June 2024).
3. Mohammadi, K.; Goudarzi, N. Association of direct normal irradiance with El Niño Southern Oscillation and its consequence on concentrated solar power production in the US Southwest. *Appl. Energy* **2018**, *212*, 1126–1137. [CrossRef]
4. Wild, M. Global dimming and brightening: A review. *J. Geophys. Res. Atmos.* **2009**, *114*, D00D16. [CrossRef]
5. Wild, M. Decadal changes in radiative fluxes at land and ocean surfaces and their relevance for global warming. *WIREs Clim. Chang.* **2016**, *7*, 91–107. [CrossRef]
6. Yuan, M.; Leirvik, T.; Wild, M. Global Trends in Downward Surface Solar Radiation from Spatial Interpolated Ground Observations during 1961–2019. *J. Clim.* **2021**, *34*, 9501–9521. [CrossRef]
7. Hatzianastassiou, N.; Ioannidis, E.; Korras-Carraca, M.-B.; Gavrouzou, M.; Papadimas, C.D.; Matsoukas, C.; Benas, N.; Fotiadi, A.; Wild, M.; Vardavas, I. Global dimming and brightening features during the first decade of the 21st century. *Atmosphere* **2020**, *11*, 308. [CrossRef]
8. Perdigão, J.C.; Salgado, R.; Costa, M.J.; Dasari, H.P.; Sanchez-Lorenzo, A. Variability and trends of downward surface global solar radiation over the Iberian Peninsula based on ERA-40 reanalysis. *Int. J. Climatol.* **2016**, *36*, 3917–3933. [CrossRef]
9. Bryce, R.; Carreño, I.L.; Kumler, A.; Hodge, B.M.; Roberts, B.; Brancucci Martinez-Anido, C. Consequences of neglecting the interannual variability of the solar resource: A case study of photovoltaic power among the Hawaiian Islands. *Sol. Energy* **2018**, *167*, 61–75. [CrossRef]
10. Juruš, P.; Eben, K.; Resler, J.; Krč, P.; Kasanický, I.; Pelikán, E.; Brabec, M.; Hošek, J. Estimating climatological variability of solar energy production. *Sol. Energy* **2013**, *98*, 255–264. [CrossRef]
11. Blair, N.; Dobos, A.P.; Freeman, J.; Neises, T.; Wagner, M.; Ferguson, T.; Gilman, P.; Janzou, S. System Advisor Model, SAM 2014.1.14: General Description NREL Report No. TP-6A20-61019; National Renewable Energy Laboratory: Golden, CO, USA, 1 February 2014. [CrossRef]
12. Larrañeta, M.; Moreno-Tejera, S.; Lillo-Bravo, I.; Silva-Pérez, M.A. Impact of the intra-day variability of the DNI on the energy yield of CSP plants. *AIP Conf. Proc.* **2019**, *2126*, 190009. [CrossRef]
13. Polo, J.; Téllez, F.M.; Tapia, C. Comparative analysis of long-term solar resource and CSP production for bankability. *Renew. Energy* **2016**, *90*, 38–45. [CrossRef]
14. Gueymard, C.A.; Al-Rasheedi, M.; Ismail, A.; Hussain, T. Long-Term variability of aerosol optical depth, dust episodes, and direct normal irradiance over Kuwait for CSP Applications. In Proceedings of the ISES Solar World Congress 2017—IEA SHC International Conference on Solar Heating and Cooling for Buildings and Industry 2017, Abu Dhabi, United Arab Emirates, 29 October–2 November 2017; International Solar Energy Society: Freiburg im Breisgau, Germany, 2017; pp. 75–84. [CrossRef]
15. Martín-Pomares, L.; Martínez, D.; Polo, J.; Perez-Astudillo, D.; Bachour, D.; Sanfilippo, A. Analysis of the long-term solar potential for electricity generation in Qatar. *Renew. Sustain. Energy Rev.* **2017**, *73*, 1231–1246. [CrossRef]
16. Wilcox, S.; Gueymard, C.A. Spatial and temporal variability of the solar resource in the united states. In Proceedings of the 39th ASES National Solar Conference 2010, SOLAR 2010, Phoenix, AZ, USA, 19–21 May 2010; Volume 2, pp. 1389–1409.
17. Tavares, A.M.; Conceição, R.; Lopes, F.M.; Silva, H.G. Development of a Simple Methodology Using Meteorological Data to Evaluate Concentrating Solar Power Production Capacity. *Energies* **2022**, *15*, 7693. [CrossRef]
18. Silva, H.G.; Abreu, E.F.; Lopes, F.M.; Cavaco, A.; Canhoto, P.; Neto, J.; Collares-Pereira, M. Solar Irradiation Data Processing using estimator MatriceS (SIMS) validated for Portugal (southern Europe). *Renew. Energy* **2020**, *147*, 515–528. [CrossRef]
19. *ISO 9060:1990*; Solar Energy—Specification and Classifications of Instruments for Measuring Hemispherical Solar and Direct Solar Radiation. International Organization for Standardization: Geneva, Switzerland, 2003. Available online: https://www.iso.org/standard/16629.html (accessed on 2 January 2022).

20. Merrouni, A.A.; Conceição, R.; Mouaky, A.; Silva, H.G.; Ghennioui, A. CSP performance and yield analysis including soiling measurements for Morocco and Portugal. *Renew. Energy* **2020**, *162*, 1777–1792. [CrossRef]
21. Lopes, D.; Conceição, R.; Silva, H.G.; Aranzabe, E.; Pérez, G.; Collares-Pereira, M. Anti-soiling coating performance assessment on the reduction of soiling effect in second-surface solar mirror. *Sol. Energy* **2019**, *194*, 478–484. [CrossRef]
22. Instituto Português do Mar e da Atmosfera. Rede de Estações Meteorológicas. Available online: https://www.ipma.pt/pt/otempo/obs.superficie/ (accessed on 2 January 2023).
23. Instituto Português do Mar e da Atmosfera. Parques Meteorológicos e Equipamentos. Available online: https://www.ipma.pt/pt/educativa/observar.tempo/index.jsp?page=ema.index.xml (accessed on 2 January 2023).
24. Lopes, F.M.; Conceição, R.; Silva, H.G.; Fasquelle, T.; Salgado, R.; Canhoto, P.; Collares-Pereira, M. Short-term forecasts of DNI from an integrated forecasting system (ECMWF) for optimized operational strategies of a central receiver system. *Energies* **2019**, *12*, 1368. [CrossRef]
25. Silva, H.G.; Merrouni, A.A.; Touili, S.; Neto, J. Determination of photovoltaic hydrogen production potential in Portugal: A techno-economic analysis. *Front. Energy Res.* **2024**, *12*, 1380543. [CrossRef]
26. Engerer, N.A. ScienceDirect Minute resolution estimates of the diffuse fraction of global irradiance for southeastern Australia. *Sol. Energy* **2015**, *116*, 215–237. [CrossRef]
27. Lopes, F.M.; Conceição, R.; Silva, H.G.; Salgado, R.; Collares-Pereira, M. Improved ECMWF forecasts of direct normal irradiance: A tool for better operational strategies in concentrating solar power plants. *Renew. Energy* **2021**, *163*, 755–771. [CrossRef]
28. Cavaco, A.; Canhoto, P.; Pereira, M.C. Procedures for solar radiation data gathering and processing and their application to DNI assessment in southern Portugal. *Renew. Energy* **2021**, *163*, 2208–2219. [CrossRef]
29. *ISO 9059:1990*; Solar Energy—Calibration of Field Pyrheliometers by Comparison to a Reference Pyrheliometer. International Organization for Standardization: Geneva, Switzerland, 1990. Available online: www.iso.org/standard/16628.html (accessed on 2 January 2022).
30. Lawin, A.E.; Niyongendako, M.; Manirakiza, C. Solar irradiance and temperature variability and projected trends analysis in Burundi. *Climate* **2019**, *7*, 83. [CrossRef]
31. Lopes, T.; Fasquelle, T.; Silva, H.G. Pressure drops, heat transfer coefficient, costs and power block design for direct storage parabolic trough power plants running molten salts. *Renew. Energy* **2021**, *163*, 530–543. [CrossRef]
32. Boretti, A.; Castelletto, S. Trends in performance factors of large photovoltaic solar plants. *J. Energy Storage* **2020**, *30*, 101506. [CrossRef]
33. Lopes, F.M.; Conceição, R.; Fasquelle, T.; Silva, H.G.; Salgado, R.; Canhoto, P.; Collares-Pereira, M. Predicted direct solar radiation (ECMWF) for optimized operational strategies of linear focus parabolic-trough systems. *Renew. Energy* **2020**, *151*, 378–391. [CrossRef]
34. National Renewable Energy Laboratory. Andasol 3 CSP Project. Available online: https://solarpaces.nrel.gov/project/andasol-3 (accessed on 2 January 2023).
35. Kariuki, B.W.; Sato, T. Interannual and spatial variability of solar radiation energy potential in Kenya using Meteosat satellite. *Renew. Energy* **2018**, *116*, 88–96. [CrossRef]
36. Luque, A.; Hegedus, S. *Handbook of Photovoltaic Science and Engineering*, 2nd ed.; John Wiley & Sons, Ltd.: Hoboken, NJ, USA, 2011; ISBN 978-0-470-72169-8.
37. Todorović, D.D.; Krasić, M.S.; Jovanović, S.; Drljača, B.; Kevkić, T. A Statistical Analysis of Long-Term Grid-Connected PV System Operation in Niš (Serbia) under Temperate Continental Climatic Conditions. *Appl. Sci.* **2023**, *13*, 6229. [CrossRef]
38. Çengel, Y.A.; Boles, M.A. Exergy: A measure of Work Potential. In *Thermodynamics: An Engineering Approach*, 5th ed.; McGraw-Hill: New York, NY, USA, 2006; Chapter 8; pp. 423–485.
39. Cavaco, A.; Silva, H.; Canhoto, P.; Neves, S.; Neto, J.; Collares Pereira, M. Global Solar Radiation in Portugal and its variability, monthly and yearly. In Proceedings of the WES 2016—Workshop on Earth Sciences, Institute of Earth Sciences, Évora, Portugal, 8–10 December 2016; p. 32.
40. Comissão Europeia. Plano Nacional Energia E. In *Plano Nacional Energia E Clima 2021–2030 (PNEC 2030)*; Comissão Europeia: Brussels, Belgium, 2019; Volume 2030, pp. 1–200.

Disclaimer/Publisher's Note: The statements, opinions and data contained in all publications are solely those of the individual author(s) and contributor(s) and not of MDPI and/or the editor(s). MDPI and/or the editor(s) disclaim responsibility for any injury to people or property resulting from any ideas, methods, instructions or products referred to in the content.